Micromixing Effects in a Two-Impinging-Jets Precipitator

Amarjit J. Mahajan and Donald J. Kirwan
Center for Bioprocess Development, Dept. of Chemical Engineering, University of Virginia, Charlottesville, VA 22903

To carry out rapid precipitation on a practical scale, the use of a two-impinging-jets (TIJ) mixer was explored in terms of its ability to deliver rapid micromixing. The two-step Bourne reaction scheme between 1-naphthol and diazosulfanilic acid was used to characterize micromixing in the TIJ mixer as a function of hydrodynamics and mixer geometry. The characteristic time for micromixing in this device was at least as small as 65 ms. The larger the jet diameter, the higher the jet Reynolds number required to achieve the same micromixing quality. The micromixing time in the TIJ mixer correlated well as a function of a Damkohler number that led to a scale-up criterion giving an inverse relationship between the micromixing time constant and the 1.5 power of the jet velocity. Finally, the precipitation of Lovastatin was carried out in the TIJ mixer under well and poorly micromixed conditions. The level of micromixing in the precipitator affected the crystal size distribution of the precipitated product only when the time constant for micromixing was comparable to or larger than the induction time for nucleation of the solute.

Introduction

Industrial precipitation of both inorganic and organic chemicals typically involves mixing two liquid streams to create supersaturation. The time required to obtain a homogeneously mixed supersaturated system depends upon the mixing technique employed. The mixing time is not a major concern in the design of a precipitation process when the precipitation kinetics are much slower than the time scale of mixing; however, this is seldom the case for most salting out and antisolvent-induced precipitations that are very rapid and occur under high supersaturation conditions. In such precipitations, a lack of rapid mixing in the precipitator can drastically affect the properties of the end product including particle size distribution (PSD), morphology, and purity.

The role of macro- and micromixing in precipitation has been identified by several researchers. Various mixing models (Becker and Larson, 1969; Pohorecki and Baldyga, 1983; Garside and Tavare, 1985; Tavare, 1986; Fitchett and Tarbell, 1990; Marcant and David, 1991; David and Marcant, 1994; Iyer and Przybycien, 1994) have been proposed and computed for continuous and semibatch stirred-tank precipitators. Design factors such as feed addition mode, feed rate, feed location, feed concentration, stirring speed, and stirrer type have been shown to affect the resulting average particle size (Kuboi et al., 1986; Mersmann and Kind, 1988; Stavek et al., 1988; Tosun, 1988; Aslund and Rasmuson, 1992). It becomes quite clear from these studies that the localized supersaturation gradient in stirred-tank precipitators is the single most important factor that controls the final PSD by influencing the nucleation and growth rates of particles. Therefore, it is believed that the mixing effects in rapid precipitation can be minimized by making the timescale of micromixing shorter than the timescale of nucleation. In other words, a precipitator with very rapid micromixing would be able to provide a homogeneously supersaturated environment before the onset of any nucleation. Thus, we first need some idea about the order-of-magnitude of the nucleation time (used synonymously with induction time) for a given precipitation system, and then a precipitator design that is capable of completely micromixing the incoming liquid streams in a time shorter than that for nucleation to occur.

Correspondence concerning this article should be addressed to D. J. Kirwan.
Present address of A. J. Mahajan: Merck & Co., Inc., P.O. Box 2000, R801-106, Rahway, NJ 07065.

One way to reduce the timescale of micromixing in a precipitator is to use a mixer design that reduces the initial scale of contact between the incoming streams and dissipates energy over a smaller liquid volume. Two-impinging-jets (TIJ) mixing is one such technique in which two liquid streams in the form of narrow, coplanar jets at high velocities impinge upon each other inside a small mixing chamber. An inelastic collision between the two jets at very high relative velocity causes rapid energy dissipation in the impingement zone that controls the smallest eddy size within which molecular diffusion is needed for further micromixing. Also, the TIJ facilitates a considerably reduced initial scale and an increased area of contact between the two liquids as compared to other conventional mixing techniques.

TIJ mixers are widely used in reaction-injection-molding (RIM) processing equipment to provide good micromixing for viscous fluids. There are a number of qualitative and quantitative impingement mixing studies reported in the RIM literature (Lee et al., 1980; Tucker and Suh, 1980; Nguyen and Suh, 1986) that measure and correlate the micromixing quality in a TIJ mixer with the jet diameter and jet Reynolds number. As discussed below, however, the geometry of such mixers for RIM applications differs significantly from that employed here for nonviscous fluids.

Tamir and Kitron (1987) have reviewed other applications of the impinging-jets technique. Their emphasis was mainly on improving interfacial heat and mass transfer in gas–liquid–solid operations and not on achieving rapid micromixing in liquid–liquid operations. Researchers in the fuel combustion field have also studied the impingement of two liquid jets in detail (Heidmann et al., 1957; Dombrowski and Hooper, 1962; Dombrowski and Hooper, 1964; Hasson and Peck, 1964; Fukui and Sato, 1972; Becker and Booth, 1975). The impinging-jet atomizer is very useful in producing a spray of fuel droplets that can be combusted easily. Naturally, these studies were more focused on the film-breaking mechanism and did not particularly concentrate on the mixing of two different liquid streams.

Jet-impingement mixing is a relatively new field to researchers in crystallization and there have been limited reports published so far in this area. *T*-mixers had been used much earlier by Nielsen (1964) in nucleation experiments, and more recently by Bhandarkar et al. (1989), but they do not supply the same level of energy dissipation. Midler et al. (1989, 1994) were the first researchers to test the suitability of a TIJ mixer for rapid precipitation of several pharmaceutical compounds. They used the mixer to contact a crude product-containing stream with precipitant and then fed the resulting mixture to an aging vessel kept stirred by an Intermig impeller. The residence time in the jet mixer was about one second, during which time the solute was precipitated either as crystals or as uniform amorphous droplets, depending on the nature of the solute. In the latter case, an amorphous-to-crystalline transformation took place in transfer lines and in the aging vessel. They concluded that the mixing intensity in the TIJ mixer was instrumental in rapidly achieving good micromixing and uniformly high supersaturation environment, which led to a highly reproducible final product of high surface area and superior crystallinity and purity. Liu et al. (1990) used the same design of the TIJ mixer for precipitation of a number of steroids and fungal metabolites and observed similar properties of the final crystalline product. They also estimated a characteristic micromixing time for this device from energy dissipation calculations by employing a number of crucial assumptions. To examine the interaction among micromixing, nucleation, and growth rates and the resulting particle size distribution, they varied the linear jet velocity and supersaturation ratio in different experimental runs. Although the characteristic time constants were not measured experimentally, from the relative values of their estimates they were able to rationalize the observed PSD. A broader PSD with a larger mean particle size was obtained from the experiments with higher characteristic micromixing times, whereas the experiments with higher nucleation time constants yielded a narrower PSD with a smaller mean size.

The preceding studies suggested the importance and advantages of rapid, efficient micromixing in crystallization systems involving rapid precipitation of biochemical compounds. However, no experimental quantification of the micromixing time constants and nucleation time constants were available. We have recently reported on the nucleation and growth kinetics of a number of solutes under high supersaturation conditions (Mahajan and Kirwan, 1994). In this article, we report our measurements and correlation of a characteristic time constant for micromixing in the TIJ device. These results along with previously measured nucleation induction times for the pharmaceutical, Lovastatin, are then used to interpret the observed particle size distribution upon precipitation in a TIJ precipitator. The goal of this work is to show that a relatively simple quantitative description of micromixing can provide useful interpretation and guidance on the influence of micromixing in a rapid precipitation process.

TIJ Mixer

A TIJ mixer similar to the one designed by Midler et al. (1989) was used in the present study and is shown in Figure 1. Two small-diameter, coplanar, high-velocity jets impinge head-on to form a liquid film that eventually disintegrates into small droplets. The size of the film increases with jet Reynolds number and the film itself remains vertical as long as both jets have equal momentum at the point of impingement. From preliminary experiments, it was observed that a length-to-diameter ratio (l/d) of about 10 was required for the nozzles to produce well-developed stable jets. Stainless-steel high-performance liquid chromatography (HPLC) tubing (Upchurch Scientific) 10 cm long with inside diameters of 0.5 mm were initially used as jet nozzles. The spacing between the nozzles could be changed easily by adjusting the tube fittings holding them. To probe into a possible scale-up criterion for the TIJ mixer, the jet nozzle diameter was changed by using HPLC tubing of 0.5, 1 and 2 mm. The mixer could be operated in a submerged or nonsubmerged mode depending on whether the polycarbonate mixing chamber (inside diameter = 2.54 cm) around the jet nozzles was filled with solution or not. Prior to each run, the mixing chamber was washed with a suitable solvent.

The reservoir system for delivering reactants to the TIJ mixer consisted of two, 4-L stainless-steel pressure vessels (Pope Scientific, Inc.) in a temperature bath. A pulseless flow of the two reactants was obtained by using pressurized nitrogen to force liquid out of the vessels. Pressures in the range 5

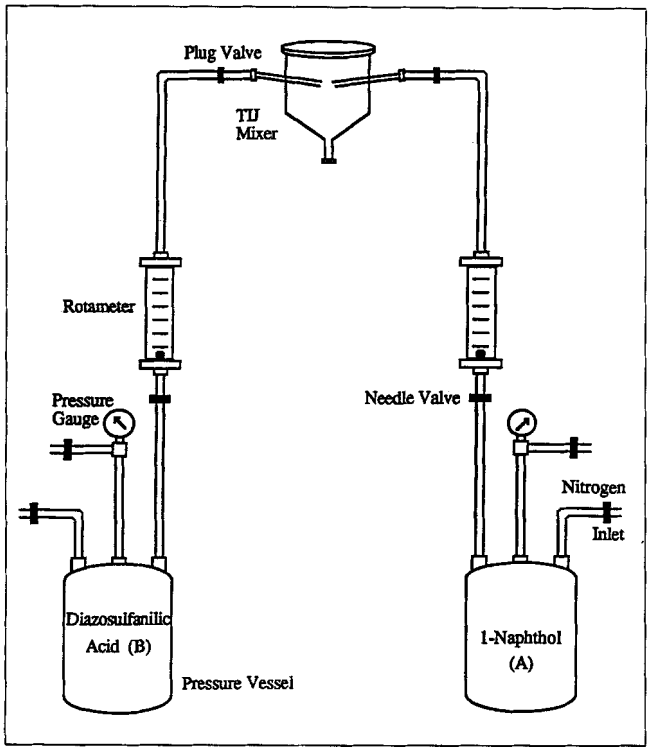

Figure 1. The TIJ mixer.

to 25 psig (34 to 172 kPa) were typically required to obtain the desired liquid flow rates that were measured with in-line rotameters (GF-1360, Gilmont Instruments). A needle valve (SS-1R4S, Whitey Co.) was used before each rotameter to change the flow rate. A plug valve (SS-4P4T, Nupro Co.) was placed in the flow line just before the jet nozzle and was used as an on/off valve to start or stop the liquid flow to the TIJ mixer. The same mixer setup was used for micromixing characterization and for precipitation experiments.

Characterization of Micromixing

Theory

Macromixing involving flow, turbulence, and eddy diffusion rapidly reduces the scale of segregation down to the Kolmogoroff microscale, after which molecular diffusion, the ultimate mechanism of micromixing, takes over to achieve a complete homogeneity. Liu et al. (1990) therefore employed a commonly used characteristic time constant for micromixing, t_M, as the time for diffusion across a slab with thickness equal to the Kolmogoroff length, λ (Demyanovitch and Bourne, 1989):

$$t_M = \frac{(0.5\,\lambda)^2}{D}. \tag{1}$$

As will be justified in a later section this formulation does not take into account laminar stretching phenomena (e.g., Bourne, 1982) that would further reduce the characteristic length over which diffusion must occur to complete the mixing process.

The Kolmogoroff length, the smallest eddy dimension, depends on the rate of energy dissipation per unit mass in turbulent mixing, ϵ, according to

$$\lambda = \left[\frac{\nu^3}{\epsilon}\right]^{1/4}, \tag{2}$$

where ν is the kinematic viscosity of the liquid. Hence, the higher the rate of energy dissipation in the mixer, the smaller is the Kolmogoroff length, resulting in faster micromixing. The rate of energy dissipation per unit mass, ϵ, can be written as

$$\epsilon = \frac{P}{\rho V}, \tag{3}$$

where P is the rate of energy dissipation, ρ is the density of liquid, and V is the volume of liquid over which the energy is dissipated. Estimates of both P and V are specific to the particular mixer geometry used.

For the TIJ mixer geometry, Liu et al. (1990) assumed P to be

$$P = \frac{1}{2}(m_1 u_1^2 + m_2 u_2^2), \tag{4}$$

that is, the kinetic energies of the two jets are assumed to be totally dissipated in an inelastic collision. When the TIJ mixer is operated in the nonsubmerged mode, a stable liquid film is obtained at the point of impingement. For the impingement angle of 160° between the two jets used in the present study, Dombrowski and Hooper (1964) have measured the film velocity to be only about 30% of the jet velocity, which supports the assumption of an inelastic collision as a first approximation to the energy dissipation calculation.

Equal momentum of the two jets is required at the point of impingement to keep the film vertical and centered between the jets. This assumption was validated experimentally using liquids of different physical properties (2-propanol and water) for the two jets. This requirement may be written as

$$m_1 u_1 = m_2 u_2 \tag{5}$$

or

$$\frac{d_1}{d_2} = \frac{Q_1}{Q_2}\left(\frac{\rho_1}{\rho_2}\right)^{0.5}. \tag{6}$$

Combining Eqs. 4, 5, and 6, we get

$$P = \frac{\pi}{8}\frac{Re_1^3 \rho_1 \nu_1^3}{d_1}\left(1 + \frac{m_1}{m_2}\right). \tag{7}$$

If the physical properties (ρ and ν) of the two jets are assumed to be equal, then combination of Eqs. 1, 2, 3 and 7 gives the following proportionality for the micromixing time constant t_M:

$$t_M \propto \frac{d_1^{0.5} V^{0.5}}{Re_1^{1.5}\left(1+\frac{m_1}{m_2}\right)^{0.5}}. \tag{8}$$

The case involving two jets of different physical properties will be considered in the discussion of our precipitation experiments.

Equation 8 can be used to predict the relationship among t_M, d, and Re for a TIJ mixer provided the dependence of the mixing zone volume, V, on jet diameter, d, or other variables is known. If V is represented by

$$V \propto d^x, \tag{9}$$

where $0 \le x \le 3$, then Eq. 8 can be rewritten as

$$t_M \propto \frac{d_1^{(x+1)/2}}{Re_1^{1.5}}. \tag{10}$$

The characteristic time constant for micromixing is sensitive to the dependence of the mixing volume, V, on jet diameter as shown in Eq. 9. Liu et al. (1990) assumed $x = 3$ and estimated the micromixing time constant to be 0.3 and 0.9 ms, respectively, for flow rates of 4.1 and 1.5 L/min through 3.17-mm-dia. nozzles, but they made no measurements of micromixing times. Experimental measurements of micromixing times can be used to verify Eq. 10 and establish the dependence of the impingement volume on diameter, that is, the value of x.

Test reaction scheme

A review of the existing mixing literature shows that a homogeneous competitive-consecutive (series-parallel) reaction scheme of the type

$$A + B \rightarrow R \quad \text{Rate Const: } k_1$$
$$R + B \rightarrow S \quad \text{Rate Const: } k_2 \ll k_1$$

is most commonly used to characterize the micromixing. Typically, B is the limiting reactant. Since the second reaction that forms the secondary product S is considerably slower than the first reaction, the characteristic reaction time constant t_R for such a reaction scheme can be assumed equal to the pseudo, first-order time constant of the second reaction, $1/k_2 C_{B0}$, where C_{B0} is the initial concentration of B after mixing. The product distribution of such a scheme will be affected significantly by the level of micromixing in the system only if $t_R \le t_M$.

The amount of S formed is typically regarded as a measure of the degree of segregation in the mixer. The distribution of B between R and S is defined as the selectivity X,

$$X = \frac{2C_S}{C_R + 2C_S}, \tag{11}$$

where C_R and C_S are the final concentrations of R and S in the reaction mixture. $X \rightarrow 0$ implies very rapid and efficient micromixing, whereas the other limit of $X \rightarrow 1$ corresponds to poor micromixing.

Bourne et al. (1981) proposed an electrophilic aromatic substitution reaction between 1-naphthol (A) and diazotized sulfanilic acid (B) to produce monoazo dye (R) and bisazo dye (S). This system has been used commonly in recent mixing studies (Tosun, 1987; Mehta and Tarbell, 1987; Andrigo et al., 1988; Demyanovich and Bourne, 1989; Kusch et al., 1989; Bourne and Hilber, 1990; Wenger et al., 1992; Iyer and Pryzbycien, 1994) since the kinetics of this reaction are well characterized (Bourne et al., 1985). The rate constants are given as $k_1 \approx 12{,}000$ m^3/mol·s and $k_2 \approx 2$ m^3/mol·s at 25°C. This scheme has been typically carried out at 25°C with $C_{B0} = 0.025$–0.05 mM, which gives t_R of about 10–20 s. The product concentrations in the reaction mixture are determined spectrophotometrically. The preceding Bourne reaction scheme was used in the present study of micromixing in the TIJ device; however, adjustments in the reaction conditions were necessary to probe the small mixing times in this device.

Experimental studies

Calculated amounts of 1-naphthol (Fisher Scientific) and diazotized sulfanilic acid (Fluka Chemicals) were dissolved in deionized, distilled water to make the reactant solutions. Since 1-naphthol does not dissolve readily in water, it had to be stirred overnight in the dark because of light sensitivity. Just prior to a run, this solution was buffered with sodium carbonate–sodium bicarbonate (10 mol/m^3) buffer to give a pH of 10. The actual concentration of diazotized sulfanilic acid in the solution was adjusted in such a way that the ratio of the concentration of 1-naphthol to that of diazotized sulfanilic acid after mixing, C_{A0}/C_{B0}, remained constant at about 1.4.

Typically, the feed vessels were charged with 1 L of the respective reactant solutions about an hour before the start of an experiment. During this time, the reactant solutions would equilibrate to 25°C. The vessels were then pressurized and the needle valves were adjusted such that the desired flow rate of the reactants was obtained. Since both reactant streams were dilute, aqueous solutions with essentially identical physical properties, equal flow rates were used for both streams to obtain a vertical impingement film. The two reactant jets would impinge head-on in the TIJ mixer and the resulting stream leaving the mixing chamber was collected for further analysis. The plug valves were then used to stop the flow of the reactants while the spectrophotometric analysis of the sample was being carried out. On its completion, a new sample was obtained by turning the plug valves on and by changing the flow rate to a new value. Typically, five or six different flowrates were investigated in every run to study micromixing time as a function of jet Reynolds number at a given jet diameter.

In an experimental run, the TIJ mixer was operated in one of two modes, submerged or nonsubmerged. In the submerged mode, the outflow from the mixing chamber was restricted so as to build up and maintain a steady liquid level above the jet nozzles. Thus, the liquid jets had to pass through the surrounding reactive mixture prior to impingement. No vertical impingement film was observed in this case. To en-

Table 1. Experimental Conditions for Micromixing Study

Mode of Oper.	Jet Nozzle Dia. d (mm)	Internozzle Spacing z (mm)	Temp. T (°C)	C_{B0} (mM)	$\frac{C_{A0}}{C_{B0}}$
N	0.5	10	25	0.025	1.39
N	0.5	10	25	0.268	1.42
N	0.5	10	25	2.35	1.46
S	0.5	10	25	2.27	1.42
S	0.5	10	25	0.245	1.44
S	0.5	10	25	0.027	1.31
N	1	10	25	0.0239	1.44
N	1	10	25	2.36	1.34
S	1	10	25	2.295	1.44
S	2	10	25	2.315	1.42
S	0.5	10	25	2.28	1.43
S	0.5	5	25	2.335	1.41
S	2	20	25	2.29	1.41
S	2	20	35	4.63	1.03
S	0.5	5	35	4.7	1.02
S	2	20	35	1.45	1.30
S	2	20	35	4.63	1.04
S	2	20	35	4.4	1.02
S	0.5	5	35	4.7	1.03
N	0.5	5	35	4.31	1.06
N	1	10	35	4.71	1.04
N	2	20	35	4.66	1.04
S	1	10	35	4.72	1.03

N—Nonsubmerged; S—Submerged.

sure a steady state, a sample was obtained at the outlet after about five residence times had elapsed. In the nonsubmerged mode, there was neither restriction on the outflow nor accumulation of the reactive mixture in the mixing chamber. As a result, the liquid jets could freely impinge to give a vertical impingement film.

To probe into a possible scale-up criterion, three different diameter jet nozzles, 0.5, 1 and 2 mm, were used, the rest of the procedure remaining the same. The effect of internozzle spacing on the micromixing also was investigated. In order to achieve faster reaction kinetics, runs were carried out at 35°C, and with considerably higher reactant concentrations. This is further explained in the Results and Discussion section. Table 1 summarizes the various experimental conditions used in the characterization of micromixing in the TIJ mixer. The initial concentrations of A and B in the impingement zone if complete mixing occurred instantaneously are denoted by C_{A0} and C_{B0}.

The samples obtained from TIJ mixer were analyzed using a diode array spectrophotometer (Model HP 89530A). The absorbance of each sample was measured at four different wavelengths, 440, 460, 480 and 500 nm. C_R and C_S in the sample mixture were then found by linear regression using previously determined specific molar absorbances. The conversion of B was generally found to be 95–97%, which compares with that typically reported by other researchers (Bourne et al., 1985; Tosun, 1987; Demyanovich and Bourne, 1989; Wenger et al., 1992; Iyer and Przybycien, 1994). The selectivity, X, calculated from the measured values of C_R and C_S, was determined as a function of jet Reynolds number for each condition listed in Table 1.

Results and discussion

Effect of Operating Mode on Micromixing. As described earlier, the reaction scheme will be sensitive to the micromixing effects in the TIJ mixer only if the reaction time constant t_R is of the order of the micromixing time constant t_M. Initial runs were made with C_{B0} of 0.025 mM, which corresponds to a t_R ($=1/k_2C_{B0}$) of about 19 s. In both submerged and nonsubmerged operating modes, the measured values of X were about 0.03 and independent of Reynolds number. This observed lower limit of 0.03 is approximately the resolution limit of the analytical technique when taking into account the uncertainties in the multilinear regression relating concentrations to absorbance readings at the four wavelengths. The lowest Re for the nonsubmerged mode was limited by the impingement requirement of the two jets. Thus, as anticipated, under these conditions the Bourne reaction under these reactant concentrations is not fast enough to show a sensitivity to the mixing. These low concentrations of $C_{B0} \approx$ 0.025 mM have been used by other researchers to study successfully the micromixing in various mixer geometries such as the double jet stirred tank (Bourne et al., 1981) and the T-mixer (Tosun, 1987) that have much longer mixing times (seconds).

One way to reduce the t_R of the reaction scheme to improve its sensitivity is to use as large a value of C_{B0} as possible (Demyanovich and Bourne, 1989). Although diazosulfanilic acid is highly soluble in water, the highest C_{B0} that can be used is limited by the solubility of 1-naphthol (A) in water at 25°C, which was observed to be about 7 mM in the present study. Therefore, the concentration of diazosulfanilic acid was increased to $C_{B0} \approx 2.5$ mM, which corresponds to $t_R \approx 200$ ms at 25°C for further experimental work. Figure 2 presents the measured values of X using this higher C_{B0} for both operating modes. In general, the reproducibility of these selectivity measurements was 2–3% when the same reagent solutions were used and 5–10% between experiments conducted with different batches of reagents. In both modes of operation there is a relatively rapid increase in X at a particular value of Re corresponding to the micromixing time becoming comparable to and then larger than the reaction time. The theoretical lowest value of X that would be attained un-

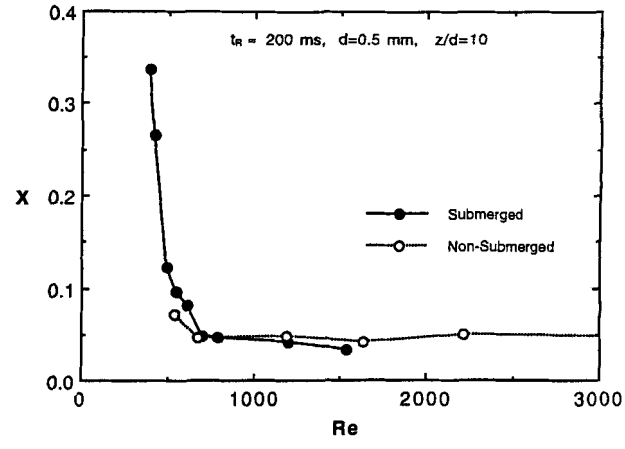

Figure 2. Selectivity measurements in the TIJ mixer with $C_{B0} \approx 2.5$ mM.

der the perfectly mixed limit can be computed from the reaction kinetics to be about 0.0003. Due to the uncertainty involved in the analytical measurements and the linear regression of the data, such low values of X could not be detected. Still, it can be concluded from the asymptotic behavior of X in Figure 2 that the micromixing time in the TIJ mixer under both operating modes is less than 200 ms for $Re > 700$.

At lower Re, the poorer micromixing observed in the case of the submerged operating mode can be explained qualitatively on the basis of a different impingement mechanism. In the nonsubmerged mode, the two narrow, cylindrical jets impinge head-on, and there is no loss of jet velocity prior to impingement. The selectivity X measured under this operating mode is thus determined mainly by the degree of segregation in the impingement zone alone. On the other hand, in the submerged mode, both jets entrain the surrounding reacting mixture and assume a roughly conical shape before their actual impingement with each other. At very small Reynolds numbers there may be no impingement at all. Therefore, the degree of segregation in *both* the entrained liquid volume and in the impingement zone of the two jets can influence the values of X measured under the submerged mode of operation. Thus, both micromixing and macromixing are involved in the process at lower Reynolds numbers. As the jet Re increases, the jet entrainment prior to impingement gradually becomes negligible, and the behavior of the submerged jets tends to approach that of the nonsubmerged jets. Therefore, for a given internozzle distance, the difference between the two modes can be assumed insignificant at higher Re. This regime at higher Re is, of course, dependent on the reaction kinetics.

Effect of Mixer Geometry on Micromixing. The effect of jet diameter on micromixing in the TIJ mixer is shown in Figure 3a. The TIJ mixer was operated in the submerged mode with a $t_R \approx 200$ ms. Three different jet nozzles with diameters of 0.5, 1 and 2 mm were used. In each run, both jet nozzles had the same diameter and the ratio of the internozzle distance, z, to the jet diameter was kept constant at 10. The results in Figure 3a show that, for a given Re, the micromixing quality decreases with increasing jet diameter, or a higher Re number is required to maintain the same micromixing at larger diameters. The latter interpretation results from a *breakpoint analysis* of the X vs. Re curves (location where X significantly deviates from the baseline asymptotic value achieved at high Re). In Figure 3a at higher Re, a flat profile for each jet diameter corresponds to $t_R \gg t_M$. As the Reynolds number decreases, the micromixing becomes poorer and t_M increases. It should be kept in mind that only t_M depends on Re, whereas t_R is fixed once C_{B0} and temperature are fixed. Finally, in a particular Re region, t_M becomes approximately equal to t_R and X starts to deviate from the horizontal asymptote. Therefore, it is assumed that the breakpoint for each jet diameter in Figure 3a corresponds to $t_M \approx 200$ ms. The breakpoint analysis facilitates an easy estimate of a micromixing time scale from the selectivity measurements. A full description of the behavior of the selectivity over the entire range of Reynolds numbers requires a model that can describe the interaction of micromixing and kinetics in the TIJ device. Further, as discussed earlier for the submerged jet operation, the macromixing associated with entrainment of surrounding fluid by the jets introduces an additional factor, dependent upon geometry and hydrodynamics, which would affect the selectivity curve as a function of Re. That is, t_M alone would not be sufficient to describe the entire curve. The complete description of the interaction of micromixing, macromixing in the case of the submerged jet, and the chemical kinetics is beyond the scope of the present investigation, where we are concerned with obtaining an estimate of the boundary points where micromixing is of importance.

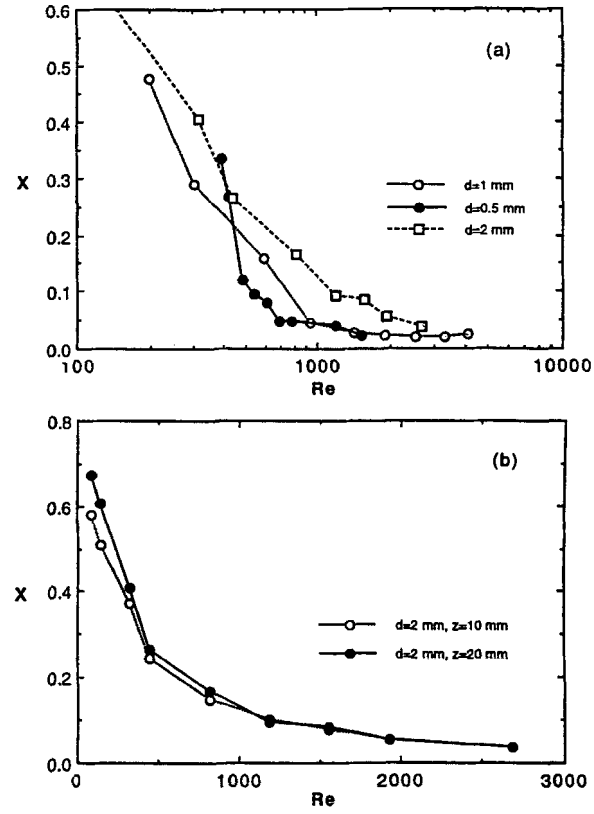

Figure 3. Effect of geometry on micromixing in the TIJ mixer in the submerged mode ($C_{B0} \approx 2.5$ mM, $T = 25$°C).

(a) Effect of nozzle diameter. (b) Effect of internozzle spacing.

Figure 3b shows the effect of internozzle distance z on micromixing with a jet diameter of 2 mm. The TIJ mixer was again operated in the submerged mode with $t_R \approx 200$ ms. At a given Re, X increases with increasing z; however, the dependence is very weak over the range of internozzle distances examined. Similar trends were observed for the other jet diameters. Therefore, for all practical purposes, the micromixing in the TIJ mixer can be assumed to be independent of the internozzle distance z as long as the two jets do impinge upon each other.

Improved Sensitivity of the Bourne Reaction. The experimental runs to this point were conducted with $C_{B0} \approx 2.5$ mM corresponding to a characteristic reaction time $t_R \approx 200$ ms; however, the reaction kinetics are too slow to be sensitive to micromixing in the nonsubmerged mode as seen from the flat profile in Figure 2. Therefore, it was decided to try to reduce t_R further by increasing k_2 and C_{B0} by carrying out the reaction at 35°C instead of 25°C since both the rate constant and

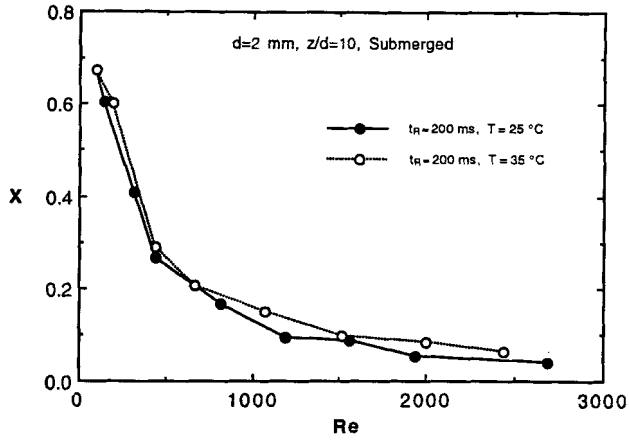

Figure 4. Confirmation of temperature dependency of Bourne reaction scheme.

the solubility increase with temperature. Table 2 reports the rate constant k_2 measured by Bourne et al. (1985) at the two temperatures. Again, the highest C_{B0} that could be used was limited by the solubility of 1-naphthol (A) at 35°C as given in Table 2. In addition to the temperature change, the ratio C_{A0}/C_{B0} was lowered from 1.4 at 25°C to 1.03 at 35°C to allow a large value of C_{B0}. Although Bourne et al. had reported the temperature dependence of k_2, the reaction at higher temperatures had not been previously used for micromixing studies. Therefore, it was considered necessary to confirm the temperature dependence of the reaction kinetics by carrying out two experimental runs at 25 and 35°C with correspondingly different C_{B0} such that both runs had the same t_R of about 200 ms. The selectivity measurements from both runs are plotted in Figure 4. The good agreement between the two curves validates the value of the kinetic constant at the higher temperature reported in Table 2. Therefore, experimental runs were now carried out at 35°C to achieve a lower value of $t_R \approx 65$ ms. An attempt to reduce t_R further by further increasing the operating temperature was unsuccessful because of the decomposition of diazosulfanilic acid as detected by shifted peaks in the absorption spectrum.

Figures 5a and 5b present the selectivity measurements at 35°C with the submerged and nonsubmerged jets, respectively. The higher values of X obtained for the nonsubmerged jets show that the reaction kinetics at 35°C are now fast enough to be sensitive to the more rapid micromixing in this operating mode. For both operating modes, the micromixing quality is seen to improve with decreasing jet diameter, which is consistent with that observed in Figure 3. It can also be noted that for each jet diameter, the breakpoint shifts to a higher Re in Figure 5a as compared to the corresponding values in Figure 3a. This again confirms that the reaction kinetics are indeed faster at 35°C than at 25°C, and can be used to measure the smaller values of t_M at higher Re. Thus, the sensitivity of the two-step Bourne reaction scheme was

Table 2. Effect of Temperature on Reaction Conditions

T(°C)	k_2 (m³/mol·s)	C_{A0} (mM)	C_{B0} (mM)	t_R (ms)
25	2.07	3.5	2.5	200
35	3.3	4.85	4.7	65

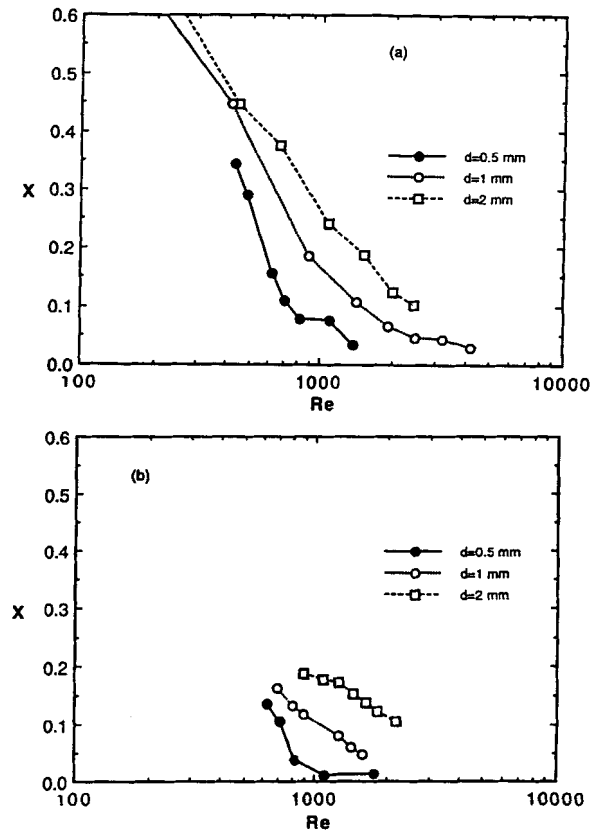

Figure 5. Effect of nozzle diameter on micromixing in the TIJ mixer ($C_{B0} \approx 4.7$ mM and $T=35$°C).
(a) Submerged jets. (b) Nonsubmerged jets.

successfully extended to probe the time scale for micromixing in the TIJ device. The selectivity measurements discussed qualitatively so far are fit to the simple Kolmogoroff theory using the breakpoint analysis in the following section.

Analysis of Micromixing Results using Kolmogoroff Theory. Earlier, a theoretical development for micromixing time in the TIJ mixer was carried out using the Kolmogoroff eddy size, which led to a relationship between the micromixing time constant, jet diameter, and Reynolds number as given by Eq. 10, which may be rewritten as

$$t_M \propto \frac{d^{(x+1)/2}}{Re^{1.5}}, \tag{12}$$

where x depends upon the relationship between impingement volume and jet diameter. The range of values of x is presumed to be between 0 and 3. The proportionality constant that would be in Eq. 12 is a function of liquid properties. The selectivity measurements presented so far can be plotted according to Eq. 12 to extract the value of x that best describes the micromixing behavior in the TIJ mixer.

The nonsubmerged jets maintain their cylindrical shape due to the lack of any entrainment until they reach the plane of impingement. As a result, the impingement zone volume is better defined in the nonsubmerged mode. Therefore, Eq. 12 will be first applied to the measured selectivity, X, plotted

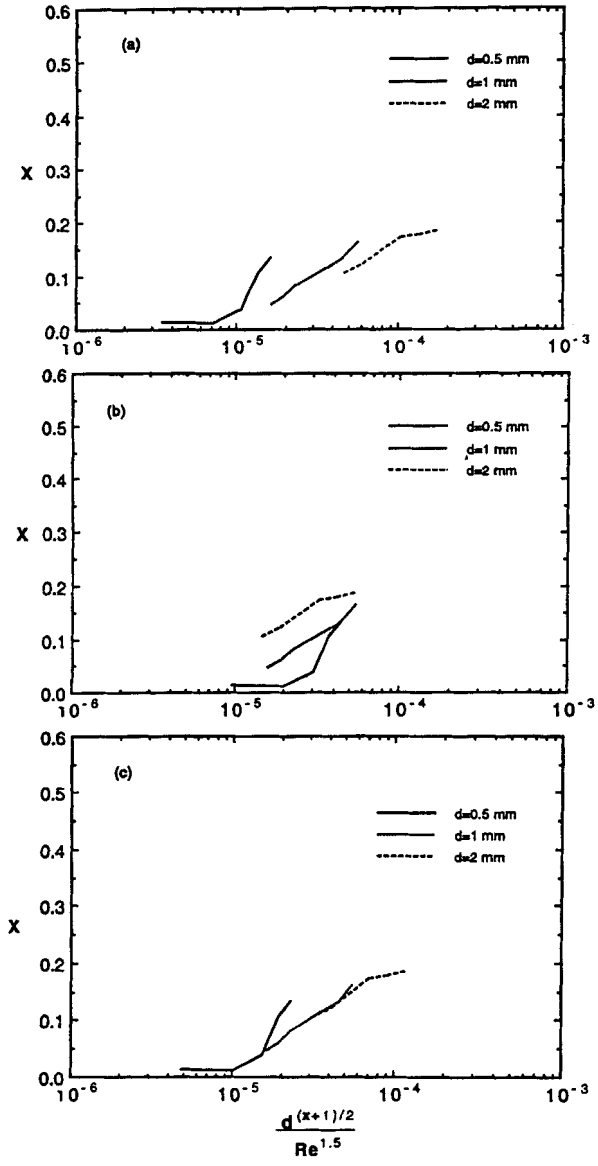

Figure 6. Correlation for micromixing in the TIJ mixer with nonsubmerged jets ($C_{B0} \approx 4.7$ mM and $T = 35$°C).

(a) $x = 3$. (b) $x = 0$. (c) $x = 2$.

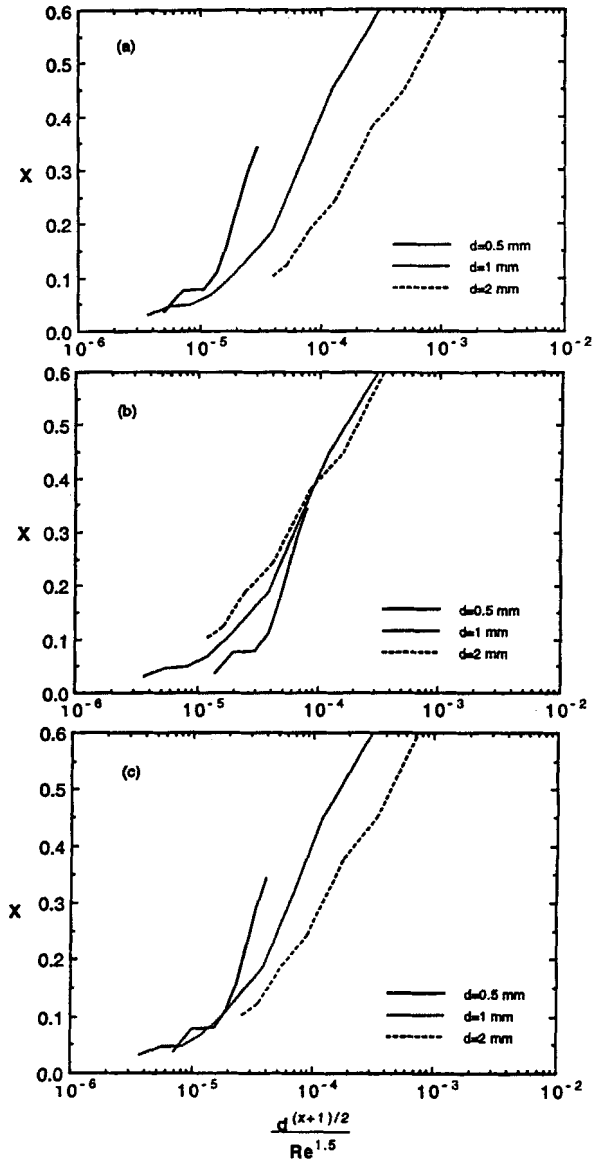

Figure 7. Correlation for micromixing in the TIJ mixer with submerged jets ($C_{B0} \approx 4.7$ mM and $T = 35$°C).

(a) $x = 3$. (b) $x = 0$. (c) $x = 2$.

against Re for nonsubmerged jets given in Figure 5b. As seen previously, the breakpoints corresponding to $t_M = t_R \approx 65$ ms were observed to be different for different jet diameters. Equation 12 suggests that these breakpoints coincide when X is replotted as a function of $d^{(x+1)/2}/Re^{1.5}$ with an appropriate value of x. This is tested in Figure 6a and 6b by replotting the data of Figure 5b with $x = 3$ ($V \propto d^3$) and $x = 0$ (V independent of d), respectively. It can be seen that the curves (and hence, breakpoints) for different diameters do not come together in either case. Therefore, both values of x can be considered inapplicable to the micromixing measurements in the TIJ mixer. By trial and error, $x = 2$ was found to give the best result as shown in Figure 6c. Although the breakpoints were not directly observed for $d = 1$ and 2 mm, it is easy to extrapolate the observations to the baseline. Further, the entire curves seem to coincide when $x = 2$, as they should if the relevant mixing process can be described with a single parameter, t_M. Therefore, the form of Eq. 12 that is followed by the experimental measurements with nonsubmerged jets in the TIJ mixer is

$$t_M \propto \left(\frac{d}{Re}\right)^{1.5} \propto \frac{1}{u^{1.5}}, \tag{13}$$

where u is the linear jet velocity.

Equation 12 can now be applied to the selectivity measurements with submerged jets. Figures 7a and 7b present the submerged mode data of Figure 5a ($t_R = 65$ ms) replotted against $d^{(x+1)/2}/Re^{1.5}$, with $x = 3$ and $x = 0$, respectively. Fig-

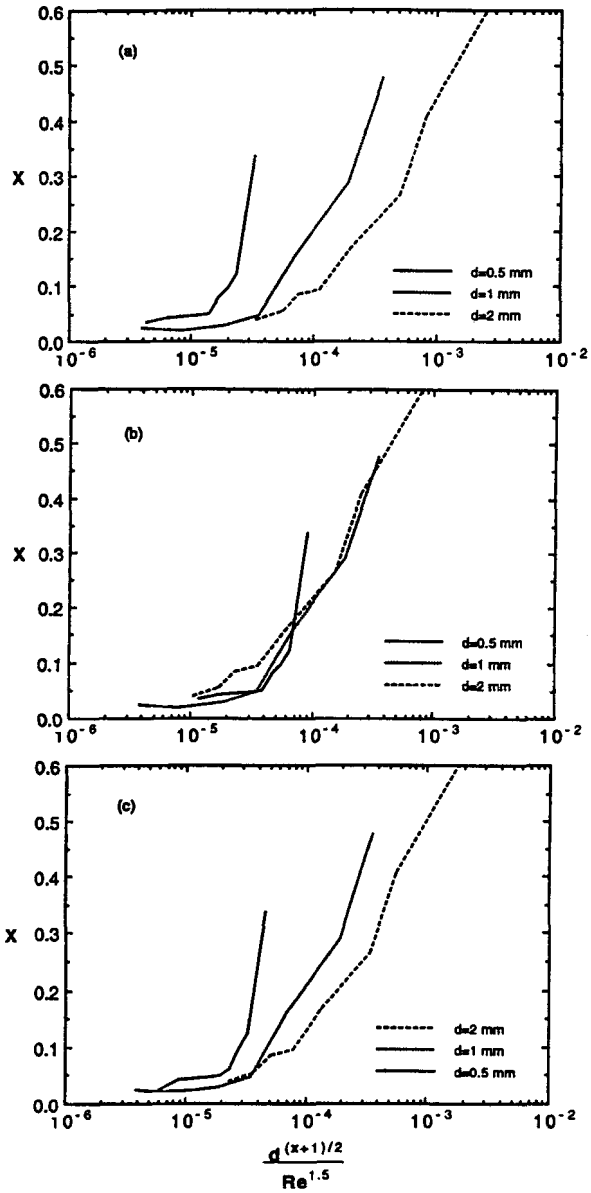

Figure 8. Correlation for micromixing in the TIJ mixer with submerged jets ($C_{B0} \approx 2.5$ mM and $T = 25$°C).

(a) $x = 3$. (b) $x = 0$. (c) $x = 2$.

ure 7b shows a good agreement between the three curves at lower *Re* (higher $d^{0.5}/Re^{1.5}$). At such low *Re* (where the two jets barely touch each other), there is an excessive entrainment of surrounding liquid into the submerged jets, and the impingement zone volume tends to equal the volume of the mixing chamber irrespective of the jet diameter. This explains the good agreement between the selectivity curves for different diameters at lower *Re* in Figure 7b, which plots the data assuming that V is independent of d ($x = 0$). However, at higher *Re* (where the jets do impinge), the breakpoints of the three curves do not merge because the submerged jets approach the behavior of the nonsubmerged jets for which V was earlier found to be dependent on d. Therefore, it can be concluded that Eq. 12 with $x = 0$ is inapplicable to the micromixing behavior of *impinging* submerged jets because it fails to bring together the three breakpoints in Figure 7b. The breakpoints do not merge in Figure 7a either, so $x = 3$ is not applicable to *impinging* submerged jets. A value of 2 for the exponent is again found to give a reasonable agreement between the breakpoints as shown in Figure 7c. It needs to be emphasized here that the preceding analysis based on Eq. 12 requires a merging of the breakpoints only (since breakpoints correspond to the same t_M) and not a coincidence of the complete X vs. *Re* curves. That is, the behavior in the poorly mixed region where fluid is entrained by the jets still has a dependence upon jet diameter at a given value of micromixing time.

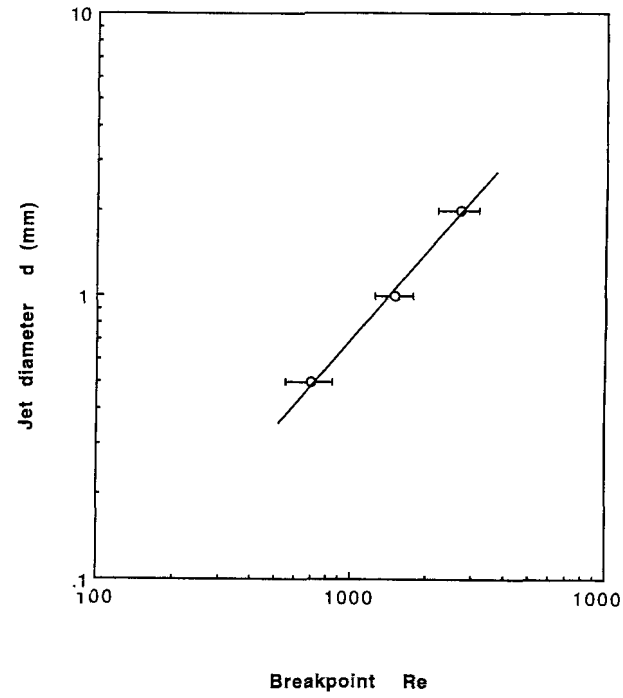

Figure 9. Breakpoint analysis of the submerged jets ($C_{B0} \approx 2.5$ mM, $T = 25$°C).

Figure 8 presents the selectivity data for the submerged jets at 25°C (cf. Figure 3a) plotted according to Eq. 12 with $x = 3$, 0, and 2, respectively. The same trends as discussed in the previous paragraph are observed in these plots. Thus, Eq. 13 is shown to hold for the *impinging* submerged jets with $t_M = t_R \approx 200$ ms as well.

The best fit value of the exponent x could also be determined by rewriting Eq. 12 as

$$\log d = K + \left(\frac{3}{x+1}\right)\log Re, \tag{14}$$

where K is a constant for a given micromixing time t_M. A log-log plot of d against the breakpoint *Re* number for the submerged jets of Figure 3a is given in Figure 9. The slope of the least squares line fit to the data is approximately unity (1.02), which again implies $x = 2$ from Eq. 14. The data from Figure 3a were chosen to examine this correlation method since the values of the breakpoints are more reliably obtained, as the curves do extend to the asymptote. Even here,

as indicated by the estimated error bars, there is a significant uncertainty using this approach. As discussed earlier, the nonsubmerged case is better analyzed by considering the coincidence of the entire X vs. Re curve.

From this discussion, it can be concluded that Eq. 13 reasonably represents the experimental micromixing data measured in the TIJ mixer under both operating modes. A corollary of this result is that the impingement zone volume V is proportional to d^2:

$$V = \frac{\pi d^2}{4} h, \tag{15}$$

where h can be considered as the effective thickness of a cylindrical micromixing region with diameter d. Since Eq. 15 is a corollary of Eq. 13, h must be independent of jet diameter and linear jet velocity. As the two jets have equal momentum at the point of impingement, h might be the interpenetration length of the two jets that Tamir (1989) has calculated to be about 10% of the internozzle distance.

It is interesting to compare the relationship in Eq. 13 with similar relationships from the RIM literature. Tucker and Suh (1980) used carbon black as a tracer and measured the mixture quality in the RIM mixhead by the light-transmittance technique. They observed a transition to turbulent mixing flow in the mixhead for nozzle Re of 140 or higher, which is about an order-of-magnitude lower than the transition Re number for turbulent flow in pipes. They derived an expression for the scale of segregation based on their measurements and the Kolmogoroff theory of turbulence. The relationship for t_M can be obtained from their result as

$$t_M \propto \frac{d^2}{Re^{1.5}}. \tag{16}$$

Nguyen and Suh (1986) used a technique that involved mixing polyurethane with an inert component, dissolving the latter with suitable solvent after gelation of polyurethane, and then, carrying out a quantitative stereological analysis of the ensuing morphology to get an idea of the scale of turbulent mixing. They found Eq. 16 to hold up well to Re number of 7,000. On the other hand, Lee et al. (1980) followed the course of impingement mixing inside a transparent RIM mixhead using high-speed photography to study qualitatively the effect of Reynolds number. They measured the mixing quality in terms of an adiabatic temperature rise due to polymerization and proposed a model based on fluid mechanical aspects of mixing such as local stretching, and on the fast and lamellar nature of the polymerization. Their result for the scale of segregation can be used to obtain t_M as

$$t_M \propto \frac{d^5}{d_m^3 Re}, \tag{17}$$

where d_m is the mixhead diameter. The disagreement between Eq. 13 and Eqs. 16 and 17 might be explained on the basis of geometrical and flow-pattern differences between a typical RIM mixer and the TIJ mixer used here. In a RIM mixer, the two jets impinge into a cylindrical mixing chamber with a diameter equal to 3–4 jet diameters and a height equal to the jet diameter. In contrast, in the TIJ device, the chamber diameter was 12–50 jet diameters and the height was 25–100 jet diameters. Also, the internozzle distance is equal to the mixhead diameter for a RIM mixer, while it was half the mixer diameter for the TIJ mixer. Unlike the TIJ mixer, a RIM mixer is not operated in the nonsubmerged mode; hence, no impingement film is formed. Unlike the RIM geometry, there is no runner following the TIJ mixer. Hence, the subsequent laminar shear stretching of the liquid mixture is absent. This is the primary reason that we based micromixing time on the simple Kolmogoroff analysis rather than including a subsequent stretching effect to further reduce the scale of segregation. Clearly, the flow patterns and the micromixing behavior in the TIJ mixer are different from those observed in a RIM mixer. The mixing chamber was considerably smaller in the RIM mixer, and the impingement volume approaches the volume of the mixing chamber itself. In the TIJ mixer, the impingement zone is not defined by the dimensions of the mixing chamber. The TIJ mixer is more similar to the jet atomizers used by the researchers in the fuels and combustion area. However, as pointed out in the introduction, those studies focused on the impingement film development/breaking mechanisms and did not particularly concentrate on the mixing of two liquid streams.

Scale-Up Criterion. Correlations for the processes involving simultaneous reaction and mixing often use a Damkohler number, Da, defined as the ratio of the characteristic micromixing time constant t_M to the characteristic reaction time constant t_R. Using the definition of t_R and the expression for t_M in Eq. 13, the Da for the TIJ mixer would be

$$Da = \frac{t_M}{t_R} \propto \frac{\left(\frac{d}{Re}\right)^{1.5}}{\left(\frac{1}{k_2 C_{B0}}\right)} \propto \frac{k_2 C_{B0}}{u^{1.5}}. \tag{18}$$

If $Da > 1$, then the micromixing is slower than the reaction kinetics, and the reaction takes place in an inhomogeneous environment. $Da = 1$ corresponds to the breakpoint, and $Da < 1$ defines the regime where the reaction is slower than the micromixing. According to Eq. 18, the breakpoints of the curves in Figures 6c and 7c for $t_R \approx 65$ ms and in Figure 8c for $t_R \approx 200$ ms should coincide when plotted against Da. This is approximately the case as shown in Figure 10. The common breakpoint does not correspond to an abscissa (Da) value of unity because the proportionality constant in Eq. 13 is missing from the scale. Indeed, from Figure 10 this constant would be of the order of 10^7. As explained before, at lower Re, the submerged jets entrain the surrounding liquid prior to impingement, which is likely to be responsible for the divergence of the various curves after the break point has been reached. At a minimum, a second Damkohler number would be needed to describe the influence of the mixing associated with entrainment on the selectivity of the reaction. Nevertheless, the results shown in Figure 10 demonstrate that we have established the hydrodynamic and geometric dependence of the micromixing time due to jet impingement.

The relationships in Eqs. 13 and 18 can readily be used to scale TIJ mixers. For example, if the jet diameter is to be

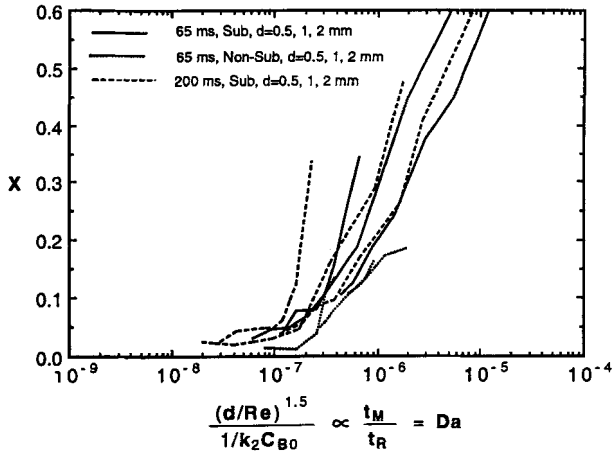

Figure 10. Reaction selectivity in the TIJ mixer as a function of Damköhler number.

increased, then, to achieve the same micromixing characteristic time at the larger scale, the same linear jet velocity needs to be maintained at the new diameter. Therefore, the volumetric throughput increases as d^2. Or, if the characteristic reaction time for a process was smaller by a factor of 6, then t_M would need to be reduced by a factor of 6 to have the same value of Da. This would require that the jet velocity u be increased by a factor of 3.3 ($= 6^{1/1.5}$). Thus, the TIJ mixer can be scaled depending upon the relevant kinetics and process scale requirements to achieve the micromixing condition suitable for the process.

In conclusion, the timescale of the micromixing in the TIJ mixer was experimentally characterized using the two-step Bourne reaction scheme. From the observed dependences of t_M on jet diameter and Re, scale-up relations were developed for micromixing in the TIJ mixer. In the following section, these practical micromixing results will be used in conjunction with fundamental precipitation kinetics data to study the rapid precipitation of Lovastatin, a pharmaceutical drug, under well-mixed and poorly mixed conditions.

Rapid Precipitation of Lovastatin in the TIJ Mixer

Experimental studies

The experimental strategy was based on the manipulation of the characteristic precipitation and micromixing time constants relative to each other to enable us to study rapid precipitation under well and poorly micromixed conditions. In particular, the effect of micromixing on the resulting particle size distribution (PSD) was observed. The precipitation of Lovastatin from methanolic solution at 25°C using water as the precipitant was chosen as the model system, as we have recently reported nucleation and growth kinetics for this system under high supersaturation conditions (Mahajan and Kirwan, 1994). The same TIJ mixer setup shown in Figure 1 was used to carry out the rapid precipitation experiments. The only difference was that in-line filters (2-μm, Balston, Inc.) were placed in the flow lines just before the jet nozzles. The TIJ mixer was operated in the nonsubmerged mode only. In the submerged mode, the crystals would settle to the bottom of the mixing chamber and would remain there partially clogging the exit port. Hence, the submerged mode was not employed due to the lack of reproducibility of the residence time of the crystals in the mixing chamber. The jet nozzle diameter was kept constant at 0.5 mm to minimize the consumption of the chemicals. The sampling of the exiting crystal slurry is explained in detail later.

It was noted earlier that the two jets need to have equal momentum at the point of impingement to form a vertical impingement film. This puts the following restriction on the jet flow rates, which is obtained from Eq. 6 for two jets of equal diameter:

$$\frac{Q_1}{Q_2} = \sqrt{\frac{\rho_2}{\rho_1}} \tag{19}$$

where Q_1, Q_2 and ρ_1, ρ_2 are the volumetric flowrates and densities of the two jets. In the rapid micromixing studies, this ratio was unity because dilute, aqueous reactant solutions were used. However, in the precipitation studies, the densities of the two streams were different, and unequal flow rates of the two streams had to be used. More specifically, the flow rate of the methanol solution was 11.2% higher than that of the primarily aqueous solution. Due to this flowrate restriction, the compositions of the feed solutions were chosen as 100% methanol and 15 vol % methanol (0.15 volume of pure methanol per 0.85 volume of water) to give a final mixture composition of 60 vol % methanol.

Typically, the two feed vessels were charged with 200 mL of solution with the preceding compositions. For each run, the amount of Lovastatin added to the methanol in the pressure vessel was based on the supersaturation ratio, C/C^*, desired for that run. The nucleation induction times, t_I, for the Lovastatin system measured previously using a novel grid mixer device (Mahajan and Kirwan, 1994) were used to select the C/C^* to be studied here. In particular, C/C^* of 8.8 and 6 were chosen corresponding to t_I of 64 and 200 ms, respectively. It should be kept in mind that the feed solution of Lovastatin in methanol was undersaturated. The preceding high supersaturation ratios were created only after mixing with the precipitant (aqueous solution) in the mixer.

Selection of the supersaturation ratios to be investigated fixed the kinetic timescale of the precipitation process. To generate well and poorly mixed conditions in the TIJ mixer relative to the Lovastatin precipitation timescale, the Reynolds numbers, Re_1 and Re_2, of the two jets were correspondingly manipulated using the micromixing characterization results of the previous section. Since the diameters of the two jets are equal, Eq. 19 can be rewritten to give the following relationship between the Reynolds numbers of the two jets:

$$\frac{Re_1}{Re_2} = \left(\frac{\rho_2}{\rho_1}\right)^{0.5} \frac{\nu_2}{\nu_1}. \tag{20}$$

Thus, once a Reynolds number is selected for one jet, the corresponding Reynolds number for the other jet is fixed by the preceding equation. Therefore, the following discussion involves the Re of just one of the two jets. From a combination of Eqs. 2, 3 and 7, the micromixing time constant t_M can be written as

$$t_m \propto \left[\frac{\bar{\rho}\bar{\nu}^3 d_2 V}{\rho_2 \nu_2^3 Re_2^3\left(1+\frac{m_2}{m_1}\right)}\right]^{0.5}, \quad (21)$$

where $\bar{\rho}$ and $\bar{\nu}$ are the density and viscosity of the liquid mixture. The subscripts 1 (solute-containing stream) and 2 (precipitant stream) are interchangeable in Eq. 21. The proportionality constant in Eq. 21 is independent of the liquid properties. Since the micromixing and precipitation studies in the TIJ mixer involved liquid streams of different properties, the results presented in the previous section about the timescale of micromixing are not directly applicable here. In other words, the t_M vs. Re trend of Figure 5b needs to be scaled appropriately using the Kolmogoroff theory analysis. To achieve the same micromixing time in the precipitation studies as in the case of the micromixing studies, from Eq. 21 we must have

$$\left[\frac{\bar{\rho}\bar{\nu}^3 d_2 V}{\rho_2 \nu_2^3 Re_2^3\left(1+\frac{m_2}{m_1}\right)}\right] = \left[\frac{\bar{\rho}\bar{\nu}^3 d_2 V}{\rho_2 \nu_2^3 Re_2^3\left(1+\frac{m_2}{m_1}\right)}\right]_{\text{micro}}, \quad (22)$$

where the lefthand side and the righthand side correspond to the precipitation and micromixing experiments, respectively.

In the micromixing studies employing the Bourne reaction scheme, both jets were made up of dilute, aqueous streams so that the properties of the liquid mixture, $\bar{\rho}$ and $\bar{\nu}$, were the same as those of the individual jets. However, in the precipitation studies, this is not true. Therefore, $\bar{\rho} \approx \rho_2$, $\bar{\nu} \approx \nu_2$, $m_1 \approx m_2$ and $Re_1 \approx Re_2 \approx Re$ can be substituted only in the right-hand side of Eq. 22, while d_2 and V are the same in both precipitation and micromixing experiments. As a result, Eq. 22 reduces to

$$\frac{\bar{\rho}\bar{\nu}^3}{\rho_2 \nu_2^3 Re_2^3\left(1+\frac{m_2}{m_1}\right)} = \frac{1}{2Re_{\text{micro}}^3}. \quad (23)$$

The liquid mixture properties $\bar{\rho}$ and $\bar{\nu}$ can be estimated as follows:

$$\bar{\rho}\bar{\nu}^3 = \frac{m_1 \rho_1 \nu_1^3 + m_2 \rho_2 \nu_2^3}{m_1 + m_2} \quad (24)$$

or

$$\frac{\bar{\rho}\bar{\nu}^3}{\rho_2 \nu_2^3} = \left(\frac{1}{1+\frac{m_2}{m_1}}\right)\frac{\rho_1}{\rho_2}\left(\frac{\nu_1}{\nu_2}\right)^3 + \left(\frac{1}{1+\frac{m_1}{m_2}}\right). \quad (25)$$

Also, from Eq. 19, m_2/m_1 can be written as

$$\frac{m_2}{m_1} = \sqrt{\frac{\rho_2}{\rho_1}}. \quad (26)$$

Table 3. Experimental Conditions for Lovastatin Precipitation

Sample No.	C/C^*	t_I (ms)	Re_2	t_M (ms)
1	5.9	200	575	145
2	5.9	200	970	65
3	8.8	65	575	145
4	8.8	65	970	65

By substitution of the appropriate values for the Lovastatin system in Eqs. 23, 25, and 26, we obtain the expression

$$Re_2 = 0.819\, Re_{\text{micro}}. \quad (27)$$

From the breakpoint analysis of Figure 5b, we find that $t_M \approx 65$ ms corresponds to $Re_{\text{micro}} \approx 1{,}200$ for $d = 0.5$ mm. Therefore, from Eq. 27, $Re_2 \approx 970$ corresponds to $t_M \approx 65$ ms in the precipitation of Lovastatin. To achieve a larger micromixing time in the TIJ mixer, a lower Re_2 of 575 was selected. Using the scale up criterion described earlier, t_M corresponding to this Re_2 was estimated. From Eq. 27, for $Re_2 = 575$, we get $Re_{\text{micro}} \approx 700$. By substitution of this value in Eq. 18, t_M was estimated as

$$\frac{t_M}{65} \approx \left(\frac{1{,}200}{700}\right)^{1.5}. \quad (28)$$

Therefore, $Re_2 = 575$ corresponded to $t_M \approx 145$ ms.

Thus, the precipitation of Lovastatin was carried out in the TIJ mixer at two different C/C^* and two different Re. The four possible combinations of the experimental conditions are given in Table 3, and correspond to conditions at which the nucleation induction time t_I is larger and smaller than the micromixing time. In each experimental run, the supersaturation ratio C/C^* was fixed at one of the two values in Table 3 at the start, and the samples were taken at the two given Reynolds numbers. Thus, samples 1 and 2 in Table 3 were obtained from a single experimental run, and samples 3 and 4 were obtained from another experimental run. The Reynolds number of the precipitant jet, Re_2, was used in Eq. 20 to obtain the proper value of Re for the solute-containing jet.

To sample the crystal slurry exiting the TIJ mixer in each of the experiments, about 0.5 mL of the suspension leaving the TIJ mixer was taken directly into 25 mL of a "quench" solution consisting of a saturated solution of Lovastatin. The saturated solution was obtained by first stirring an excess amount of Lovastatin into 60 vol % methanol for at least 24 hours and then filtering through a 0.22-μm membrane filter (Gelman Sciences). The distance from the point of impingement of the two jets to the point of collection and quenching was carefully adjusted so that, for a given C/C^*, the supersaturated crystal slurry sample had the same residence time for both Reynolds numbers before it entered the quenching solution. This time was selected to be long enough to have measurable crystal nucleation and growth. After the initial micromixing in the impingement zone of the nonsubmerged jets, the exiting crystal slurry can be thought of as forming a plug flow stream. Thus, the observed particle size distribu-

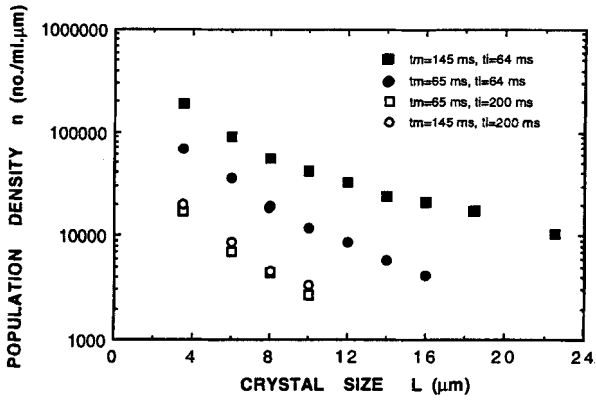

Figure 11. Effect of micromixing on the particle size distribution of Lovastatin precipitated in the TIJ mixer.

tion corresponded to the same residence time and supersaturation ratio and only the micromixing characteristics were different. In particular, at $Re_2 = 575$, the flow rates Q_1 and Q_2 were low and a quenching distance of 30 cm was used. For $Re_2 = 970$, both Q_1 and Q_2 were higher and the quenching distance used was 35.5 cm. These distances are not linear with volumetric flow rate because the exiting fluid accelerates due to gravity upon leaving the chamber. The PSD of the quenched sample was obtained using a light-obscuring particle counter (Model 4300, HIAC/ROYCO Instruments).

Results and discussion

The measured population density curves for the four conditions in Table 3 are shown in Figure 11. All four samples were quenched after equal residence times as explained earlier. Each data point shown is an average of three measurements. The size of the error bars is smaller than the size of the symbols. The four curves can be interpreted with the help of the relative magnitudes of t_I and t_M for each sample. For the lower supersaturation C/C^* of 5.9, $t_I = 200$ ms is longer than either of the micromixing times of 65 or 145 ms. Hence, the micromixing in the TIJ mixer was faster than the Lovastatin precipitation kinetics; and, as a result, the measured PSD at C/C^* of 5.9 showed no effect of Reynolds number. For these two samples, the micromixing was essentially complete before the onset of any nucleation or growth phenomenon in the TIJ precipitator, and the precipitation of Lovastatin crystals took place in a homogeneously mixed environment.

Comparison of the two curves from the experimental runs at a C/C^* of 8.8 with those at lower supersaturation shows that considerably higher values of the population density, n, are observed at the higher supersaturation ratio. Since all four samples had the same residence time before being quenched by the saturated solution, the higher values of the population density obtained over the entire size range is a consequence of the higher nucleation and growth rates of Lovastatin crystals at $C/C^* = 8.8$. In contrast to the samples at $C/C^* = 5.9$, these samples do show a micromixing effect. For the experiment at higher Re, t_M is 65 ms and t_I is about 64 ms so that the characteristic times for micromixing and nucleation are comparable. For the sample at lower Re, t_M is about 145 ms, which is significantly longer than t_I. As a result, the nucleation and growth of Lovastatin crystals had already begun before micromixing in the TIJ precipitator was complete, and the resulting population density is significantly different from that measured at the higher Reynolds number. Due to highly nonlinear nucleation and growth kinetics of Lovastatin crystals (Mahajan and Kirwan, 1994), the effect of supersaturation gradients present in the nonhomogeneous mixture was magnified and resulted in a much wider particle size distribution. These observations are consistent with the trends reported by Liu et al. (1990) for the rapid precipitation of a number of pharmaceutical drugs in a TIJ precipitator.

These results clearly demonstrated the influence of micromixing on precipitation processes. Further, having independently measured the kinetics for the process, it is possible to interpret the results in terms of the relative magnitudes of the characteristic times for micromixing and precipitation. Knowledge of the characteristic time constant for a precipitation process then allows one to specify the necessary micromixing time that must be achieved. The results presented earlier on the dependence of the micromixing time constant in the TIJ device on jet velocity would then allow one to specify the jet velocity and size for a particular throughput.

Conclusions

By modification of the Bourne reaction scheme to higher temperatures and reactant concentrations, characteristic micromixing times as small as 65 ms could be observed.

At lower Reynolds numbers (< 800), the nonsubmerged mode of operation was found to provide better micromixing, possibly because of the entrainment of surrounding liquid by submerged jets. At higher Re, entrainment becomes negligible, and the micromixing characteristics of both modes were similar.

The internozzle distance was seen to have a negligible effect on the micromixing in the TIJ mixer as long as the two jets could impinge on each other. The micromixing quality decreased in both operating modes with increasing jet diameter for a given Reynolds number. Breakpoint analysis of the selectivity plots established that the characteristic micromixing time constant was independent of jet diameter and varied as the jet velocity to the -1.5 power. This suggests that the volume in the TIJ mixer over which energy is dissipated is proportional to the square of the jet diameter.

The quantitative measurements of micromixing time in the TIJ device measured in this work along with the kinetic time constants for Lovastatin nucleation (Mahajan and Kirwan, 1994) were used successfully to interpret the CSD observed during the precipitation of Lovastatin in the TIJ mixer under different hydrodynamic conditions.

Acknowledgment

Support of this work by Manufacturing Div. of Merck & Co., Inc. is appreciated.

Literature Cited

Andrigo, P., R. Bagatin, P. Cavalieri d'Oro, C. Perego, and L. Raimondi, "Micromixing in a Chemical Quenching Apparatus for Fast Kinetics," *Chem. Eng. Sci.*, **43**, 1923 (1988).

Aslund, B. L., and A. C. Rasmuson, "Semibatch Crystallization of Benzoic Acid," *AIChE J.*, **38**, 328 (1992).

Becker, G. E., and M. A. Larson, "Mixing Effects in Continuous Crystallization," *AIChE Symp. Ser.*, **65**(95), 14 (1969).
Becker, H. A., and B. D. Booth, "Mixing in the Interaction Zone of Two Free Jets," *AIChE J.*, **21**, 949 (1975).
Bhandarkar, S., R. Brown, and J. Estrin, "Studies in Rapid Precipitation of Hydroxides of Calcium and Magnesium," *J. Crystal Growth*, **97**, 407 (1989).
Bourne, J. R., "The Characterization of Micromixing Using Fast Multiple Reactions," *Chem. Eng. Commun.*, **16**, 79 (1982).
Bourne, J. R., F. Kozicki, and P. Rys, "Mixing and Fast Chemical Reaction: I. Test Reactions to Determine Segregation," *Chem. Eng. Sci.*, **36**, 1643 (1981).
Bourne, J. R., C. Hilber, and G. Tovstiga, "Kinetics of the Azo Coupling Reactions between 1-Naphthol and Diazotized Sulphanilic Acid," *Chem. Eng. Commun.*, **37**, 293 (1985).
Bourne, J. R., and C. P. Hilber, "The Productivity of Micromixing-Controlled Reactions: Effect of Feed Distribution in Stirred Tanks," *Trans. Inst. Chem. Eng.*, **68**, 51 (1990).
David, R., and B. Marcant, "Prediction of Micromixing Effects in Precipitation: Case of Double-Jet Precipitators," *AIChE J.*, **40**, 424 (1994).
Demyanovich, R. J., and J. R. Bourne, "Rapid Micromixing by the Impingement of Thin Liquid Sheets. 2. Mixing Study," *Ind. Eng. Chem. Res.*, **28**, 830 (1989).
Dombrowski, N., and P. C. Hooper, "The Performance Characteristics of an Impinging Jet Atomizer in Atmospheres of High Ambient Density," *Fuel*, **41**, 323 (1962).
Dombrowski, N., and P. C. Hooper, "A Study of the Sprays Formed by Impinging Jets in Laminar and Turbulent Flow," *J. Fluid Mech.*, **18**, 392 (1964).
Fitchett, D. E., and J. M. Tarbell, "Effect of Mixing on the Precipitation of Barium Sulfate in an MSMPR Reactor," *AIChE J.*, **36**, 511 (1990).
Fukui, N., and T. Sato, "The Study of a Liquid Atomization by the Impingement of Two Jets," *Bull. JSME*, **15**, 609 (1972).
Garside, J., and N. S. Tavare, "Mixing, Reaction and Precipitation: Limits of Micromixing in an MSMPR Crystallizer," *Chem. Eng. Sci.*, **40**, 1485 (1985).
Hasson, D., and R. E. Peck, "Thickness Distribution in a Sheet Formed by Impinging Jets," *AIChE J.*, **10**, 752 (1964).
Heidmann, M. F., R. J. Priem, and J. C. Humphrey, "A Study of Sprays Formed by Two Impinging Jets," N.A.C.A. Tech. Note No. 3835 (1957).
Iyer, H. V., and T. M. Przybycien, "Protein Precipitation: Effects of Mixing on Protein Solubility," *AIChE J.*, **40**, 349 (1994).
Kuboi, R., M. Harada, J. M. Winterbottom, A. J. S. Anderson, and A. W. Nienow, "Mixing Effects in Double-Jet and Single-Jet Precipitation," World Cong. of Chem. Eng., Part II, Tokyo, **8g-302**, 1040 (1986).
Kusch, H. A., J. M. Ottino, and D. M. Shannon, "Analysis of Impingement Mixing-Reaction Data: Use of a Lamellar Model to Generate Fluid Mixing Information," *Ind. Eng. Chem. Res.*, **28**, 302 (1989).
Lee, L. J., J. M. Ottino, W. E. Ranz, and C. W. Macosko, "Impingement Mixing in Reaction Injection Molding," *Poly. Eng. Sci.*, **20**, 868 (1980).
Liu, P. D., M. Futran, M. Midler, and E. L. Paul, "Particle Size Design of Pharmaceuticals by Continuously Impinging Jets Precipitation," AIChE Meeting, Chicago (1990).
Mahajan, A. J., and D. J. Kirwan, "Nucleation and Growth Kinetics of Biochemicals Measured at Very High Supersaturations," *J. Crystal Growth*, **144**, 281 (1994).
Marcant, B., and R. David, "Experimental Evidence for and Prediction of Micromixing Effects in Precipitation," *AIChE J.*, **37**, 1698 (1991).
Mehta, R. V., and J. M. Tarbell, "An Experimental Study of the Effect of Turbulent Mixing on the Selectivity of Competing Reactions," *AIChE J.*, **33**, 1089 (1987).
Mersmann, A., and M. Kind, "Chemical Engineering Aspects of Precipitation from Solution," *Chem. Eng. Technol.*, **40**, 264 (1988).
Midler, M., E. L. Paul, and E. F. Whittington, "Production of High Purity, High Surface Area Crystalline Solids by Turbulent Contacting and Controlled Secondary Nucleation," Engineering Foundation Conf. on Mixing, Potosi, MO (1989).
Midler, M., E. L. Paul, E. F. Whittington, M. Futran, P. D. Liu, J. Hsu, and S. Pan, "Crystallization Method to Improve Crystal Structure and Size," U.S. Patent No. 5,314,506 (1994).
Nguyen, L. T., and N. P. Suh, "Processing of Polyurethane/Polyester Interpenetrating Polymer Networks by Reaction Injection Molding: Part II. Mixing at High Reynolds Numbers and Impingement Pressures," *Poly. Eng. Sci.*, **26**, 799 (1986).
Nielsen, A. E., *Kinetics of Precipitation*, Pergamon, Oxford (1964).
Pohorecki, R., and J. Baldyga, "The Use of a New Model of Micromixing for Determination of Crystal Size in Precipitation," *Chem. Eng. Sci.*, **38**, 79 (1983).
Stavek, J., I. Fort, J. Nyvlt, and M. Sipek, "Influence of Hydrodynamic Conditions on the Controlled Double-Jet Precipitation of Silver Halides in Mechanically Agitated Systems," Euro. Conf. on Mixing, BHRA, Pavia, Italy, p. 171 (1988).
Tamir, A., "Processes and Phenomena in Impinging-Stream Reactors," *Chem. Eng. Prog.*, **85**, 53 (1989).
Tamir, A., and A. Kitron, "Applications of Impinging-Streams in Chemical Engineering Processes—Review," *Chem. Eng. Commun.*, **50**, 241 (1987).
Tavare, N. S., "Mixing in Continuous Crystallizers," *AIChE J.*, **32**, 705 (1986).
Tosun, G., "A Study of Micromixing in Tee Mixers," *Ind. Eng. Chem. Res.*, **26**, 1184 (1987).
Tosun, G., "An Experimental Study of the Effect of Mixing on the Particle Size Distribution in $BaSO_4$ Precipitation Reaction," Euro. Conf. on Mixing, BHRA, Pavia, Italy, p. 161 (1988).
Tucker, C. L., and N. P. Suh, "Mixing for Reaction Injection Molding. I. Impingement Mixing of Liquids," *Poly. Eng. Sci.*, **20**, 875 (1980).
Wenger, K. S., E. H. Dunlop, and I. D. MacGilp, "Investigation of the Chemistry of a Diazo Micromixing Test Reaction," *AIChE J.*, **38**, 1105 (1992).

Manuscript received Nov. 7, 1994, and revision received Oct. 13, 1995.